Journal of KSNVE, Vol. 10, No. 2, pp. 353~360, 2000.

〈Original Paper〉

Free Vibrations of Tapered Cantilever Arches with Variable Curvature

變斷面 變化曲率 캔틸레버 아치의 自由振動

Byoung-Koo Lee*, Yong-Soo Lee** and Sang-Jin Oh***
이 병 구·이 용 수·오 상 진

(Received January 21, 2000 : Accepted February 27, 2000)

Key Words : Arch with Variable Curvature(變化曲率 아치), Cantilever Arch(캔틸레버 아치), Free Vibration(自由振動), Rotatory Inertia(回轉慣性), Tapered Arch(變斷面 아치)

ABSTRACT

Numerical methods are developed for calculating the natural frequencies and mode shapes of the tapered cantilever arches with variable curvature. The differential equations governing the free vibrations of such arches are derived and solved numerically, in which the effect of rotatory inertia is included. The parabolic shape is chosen as the arch with variable curvature while both the prime and quadratic arched members are considered as the tapered arch. Comparisons the natural frequencies between this study and finite element method SAP 90 serve to validate the numerical method developed herein. The lowest four natural frequencies are reported as a function of four non-dimensional system parameters. The effects of both the rotatory inertia and cross-sectional shape are reported. Also, the typical mode shapes of stress resultants as well as the displacements are reported.

要 約

이 논문은 變斷面 變化曲率 캔틸레버 아치의 自由振動에 관한 연구이다. 변단면 변화곡률 아치의 자유진동을 지배하는 常微分方程式을 유도하고 이를 數値解析하여 固有振動數와 振動形을 산출하였다. 변화곡률 아치로는 抛物線의 선형을, 변단면 아치로는 1次元 및 2次元 변단면 부재를 채택하였다. 본 연구와 SAP 90의 결과가 매우 잘 일치하여 이 연구에서 개발한 數値解析 方法의 타당성을 입증할 수 있었다. 수치해석의 결과로 無次元 固有振動數와 無次元 變數들 사이의 관계를 고찰하였다. 또한 回轉慣性과 斷面形狀이 고유진동수에 미치는 영향을 분석하고, 아치 變位와 合應力의 진동형을 그림에 나타내었다.

1. Introduction

Since arches are the basic structural forms, these units are widely used in the various engineering fields. Studies on the free vibrations of linearly elastic arches have been reported for more than three decades. Such studies were critically reviewed by Laura and Maurizi[1]. Background material for the current study was summarized by Oh, et al[2]. Briefly, such works included studies of non-circular arches with predictions of the lowest frequency in flexure by Romanelli and Laura[3], and in extension by Wang[4], and Wang and Moore[5]; Lee and Wilson[6] studied the free vibrations

* Member, Dept. of Civil and Environmental Engineering, Wonkwang University
** Dept. of Architectural Engineering, Wonkwang University
***Member, Dept. of Civil Engineering, Provincial College of Damyang

of uniform arches with variable curvature in flexure. For tapered arches, Royster[7] computed the fundamental extensional frequencies of tapered circular arches; Wang[4] computed the fundamental frequencies of parabolic arches with variable width and depth; Laura and Verniere[8] calculated the fundamental frequencies of circular arches with thickness varying in a discontinuous fashions. In the works just cited, the Rayleigh-Ritz method was used. Sakiyama[9] and Wilson, et al.[10] presented another approximate methods for analyzing the free vibrations of arches with variable cross-section. Studies showing the effect of rotatory inertia on free vibrations were investigated by Irie, et al.[11], Lee and Wilson[6], and Oh, et al.[2].

The main purpose of this paper is to present both the fundamental and some higher free vibration frequencies for the linearly elastic tapered cantilever arches with variable curvature, in which the rotatory inertia is included. The differential equations are derived in polar co-ordinates system and solved numerically. Theories and numerical methods adopted herein have the advantage of such that both the frequencies and mode shapes should be obtained without the assumption of eigenfunctions. The parabolic shape is chosen as the arch with variable curvature while both the prime and quadratic arched members are considered as the tapered arch. In the most previous works, the most end constraints of the arches are clamped-clamped, hinged-hinged and clamped-hinged. However, the numerical results concerning the cantilever arches are very rare even though its numerical data are very important when these units are used as the substructures such as the porch frames in large buildings. From this viewpoint, the clamped-free ends, namely cantilever arch, are chosen as the end constraints in this study. The lowest four natural frequencies are presented, and both the effects of rotatory inertia and cross-sectional shape on the natural frequencies are reported. In addition, the mode shapes of stress resultants as well as the deflected shapes of arch axes are illustrated.

2. Mathematical Model

The geometry and variables of an arch considered in this study are shown in Fig. 1. The shape of arch with variable curvature is $y=y(x)$ in the Cartesian co-ordinates, which is supported by the clamped-free ends, namely cantilever arch. Its chord length, span length and rise are depicted as L, l and H, respectively. At any point of arch (x, y), the area, area moment of inertia and arc length are depicted as A, I and s, respectively. The A, I and s values at free end are A_f, I_f and s_f, respectively, and the I value at clamped end is I_c. The radius of curvature is depicted as r and its inclination with x-axis is ϕ. Also the vertical and tangential displacements, and rotation of cross-section are depicted as w, v and ψ, respectively.

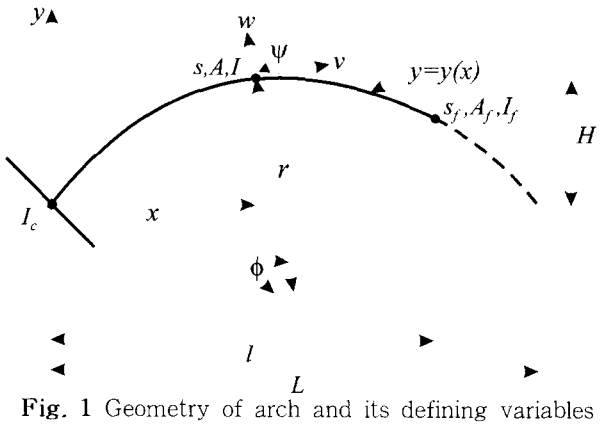

Fig. 1 Geometry of arch and its defining variables

In this study, the shape of parabolic is chosen as the arch with variable curvature. Its shape is expressed in terms of (L, H) and the co-ordinate x in the range from $x=0$ to $x=l$. That is,

$$y = -(4H/L^2)x(x-L), \quad 0 \le x \le l \tag{1}$$

The quantities A and I are expressed in the form

$$A = A_f F \tag{2}$$

$$I = I_f G \tag{3}$$

where both $F=F(s)$ and $G=G(s)$ are the functions of single variable s, as discussed in section 3.

A small element of the arch shown in Fig. 2 defines the positive directions for its loads: the axial load N; the shear force Q; the bending moment M; the radial inertia force P_r; the tangential inertia force P_t; and rotatory inertia couple T. With inertia forces and the

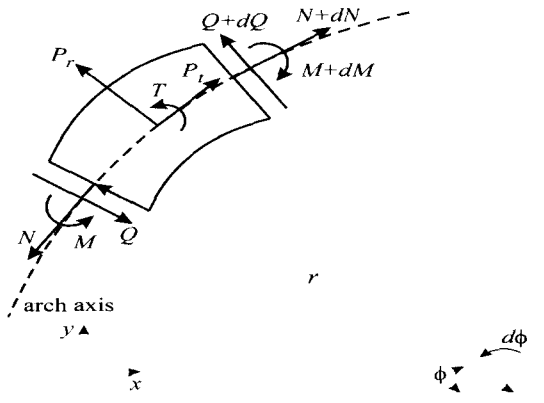

Fig. 2 Loads on a small arch element

inertia couple treated as equivalent static quantities, the three equations for "dynamic equilibrium" of the element are

$$dN/d\phi + Q + rP_t = 0 \tag{4}$$

$$dQ/d\phi - N + rP_r = 0 \tag{5}$$

$$r^{-1}dM/d\phi - Q - T = 0 \tag{6}$$

The equations N, M and ϕ that relate to the displacements w and v account for the axial deformation due to N. These equations, given by Borg and Gennaro[12], are

$$\begin{aligned} N &= E[Ar^{-1}(v'+w) + Ir^{-3}(w''+w)] \\ &= E[A_f F r^{-1}(v'+w) + I_f G r^{-3}(w''+w)] \end{aligned} \tag{7}$$

$$M = -EIr^{-2}(w''+w) = -EI_f G r^{-2}(w''+w) \tag{8}$$

$$\phi = r^{-1}(w'-v) \tag{9}$$

where each prime is one derivative with respect to ϕ and E is Young's modulus.

The arch is assumed to be in harmonic motion, or each co-ordinate is proportional to $\sin(\omega t)$ where ω is the frequency parameter and t is time. The inertia loadings per unit arc length are then

$$\begin{aligned} P_r &= \gamma A \omega^2 w \\ &= \gamma A_f F \omega^2 w \end{aligned} \tag{10}$$

$$\begin{aligned} P_t &= \gamma A \omega^2 v \\ &= \gamma A_f F \omega^2 v \end{aligned} \tag{11}$$

$$\begin{aligned} T &= \gamma I \omega^2 \phi \\ &= \gamma I_f G \omega^2 r^{-1}(w'-v) \end{aligned} \tag{12}$$

where γ is mass density of arch material and $\gamma A = \gamma A_f F$ is mass per unit arc length at any point of arch.

When Eqs. (8) and (12) are substituted into Eq. (6), then

$$\begin{aligned} Q &= r^{-1}dM/d\phi - RT \\ &= -EI_f G' r^{-3}(w''+w) - EI_f G r^{-3}(w'''+w') \\ &\quad - R\gamma I_f G \omega^2 r^{-1}(w'-v) \end{aligned} \tag{13}$$

Here $R=0$ if rotatory inertia is ignored and $R=1$ if rotatory inertia is included.

To facilitate the numerical studies, the following non-dimensional system variables are defined. First, the rise H, the span length l and the total arc length s_f are normalized by the chord length L:

$$h = H/L \tag{14}$$

$$e = l/L \tag{15}$$

$$k = s_f/L \tag{16}$$

The section ratio α and slenderness ratio λ are defined as follows.

$$\alpha = I_c/I_f \tag{17}$$

$$\lambda = L/(I_f/A_f)^{1/2} \tag{18}$$

The co-ordinates (x, y), the displacements (w, v), the radius of curvature r and the arc length s are normalized by the chord length L:

$$\xi = x/L \tag{19}$$

$$\eta = y/L \tag{20}$$

$$\delta = w/L \tag{21}$$

$$\zeta = v/L \tag{22}$$

$$\rho = r/L \tag{23}$$

$$\mu = s/L \tag{24}$$

Finally, the non-dimensional frequency parameter is defined as

$$c_i = \omega_i \lambda L(\gamma/E)^{1/2} \tag{25}$$

which is written in terms of the ith frequency $\omega = \omega_i$, $i = 1, 2, 3, 4, \cdots$.

When Eqs. (7), (10) and (13) are substituted into Eq. (5) and the non-dimensional forms of Eqs. (14) ~ (25) are used, the result is

$$\begin{aligned} \delta'''' = {} & a_1\delta''' + (a_2 + a_3 c_i^2)\delta'' + (a_4 + a_5 c_i^2)\delta' \\ & + (a_6 + a_7 c_i^2)\delta + (a_8 + a_9 c_i^2)\zeta' + a_{10} c_i^2 \zeta \end{aligned} \tag{26}$$

When Eqs. (7), (11) and (13) are substituted into Eq. (4) and the non-dimensional forms of Eqs. (14)~(25) are used, the result is

$$\zeta'' = a_{11}\delta'' + (a_{12}c_i^2 - 1)\delta' + a_{13}\delta + a_{14}\zeta' + a_{15}c_i^2\zeta \tag{27}$$

In the last two equations, the constants are as follows.

$$a_1 = -2G'G^{-1} + 5\rho'\rho^{-1} \tag{28-a}$$

$$a_2 = -2 - G''G^{-1} + 5G'G^{-1}\rho'\rho^{-1} - 8\rho'^2\rho^{-2} + 2\rho''\rho^{-1} \tag{28-b}$$

$$a_3 = -R\lambda^{-2}\rho^2 \tag{28-c}$$

$$a_4 = -2G'G^{-1} + 5\rho'\rho^{-1} \tag{28-d}$$

$$a_5 = -R\lambda^{-2}(G'G^{-1}\rho^2 - \rho'\rho) \tag{28-e}$$

$$a_6 = -1 - \lambda^2 FG^{-1}\rho^2 - G''G^{-1} + 5G'G^{-1}\rho'\rho^{-1} - 8\rho'^2\rho^{-2} + 2\rho''\rho^{-1} \tag{28-f}$$

$$a_7 = FG^{-1}\rho^4 \tag{28-g}$$

$$a_8 = -\lambda^2 FG^{-1}\rho^2 \tag{28-h}$$

$$a_9 = R\lambda^{-2}\rho^2 \tag{28-i}$$

$$a_{10} = R\lambda^{-2}(G'G^{-1}\rho^2 - \rho'\rho) \tag{28-j}$$

$$a_{11} = \lambda^{-2}GF^{-1}\rho'\rho^{-3} \tag{28-k}$$

$$a_{12} = R\lambda^{-4}GF^{-1} \tag{28-l}$$

$$a_{13} = \lambda^{-2}GF^{-1}\rho'\rho^{-3} - F'F^{-1} + \rho'\rho^{-1} \tag{28-m}$$

$$a_{14} = -F'F^{-1} + \rho'\rho^{-1} \tag{28-n}$$

$$a_{15} = -R\lambda^{-4}GF^{-1} - \lambda^{-2}\rho^2 \tag{28-o}$$

The Eqs. (26) and (27) with $\rho' = \rho'' = 0$ are reduced to governing differential equations for in-plane free vibration of tapered circular arch and these results coincide with equations of Wilson, et al.[10].

Arch stresses may be computed from the following non-dimensional forms for the normal load N, the transverse load Q and the bending moment M. The respective results, obtaining from Eqs. (7), (13) and (8) using Eqs. (14)~(25), are:

$$n = NL^2/EI_f = \lambda^2 F\rho^{-1}(\zeta' + \delta) + G\rho^{-3}(\delta'' + \delta) \tag{29}$$

$$q = QL^2/EI_f = -G\rho^{-3}(\delta''' + \delta') - (G'\rho^{-3} - 2G\rho^{-4}\rho')(\delta'' + \delta) - Rc_i^2\lambda^{-2}G\rho^{-1}(\delta' - \zeta) \tag{30}$$

$$m = ML/EI_f = -G^{-2}\rho(\delta'' + \delta) \tag{31}$$

For the clamped end at $x = 0$, the boundary conditions are $w = v = \psi = 0$ and these relations can be expressed in non-dimensional forms as

$$\delta = 0 \quad \text{at } \xi = 0 \tag{32}$$

$$\zeta = 0 \quad \text{at } \xi = 0 \tag{33}$$

$$\delta' = 0 \quad \text{at } \xi = 0 \tag{34}$$

For the free end at $x = l$, the boundary conditions are $N = Q = M = 0$ and these relations can be expressed in non-dimensional forms as

$$n = 0 \text{ at } \xi = e \tag{35}$$

$$q = 0 \text{ at } \xi = e \tag{36}$$

$$m = 0 \text{ at } \xi = e \tag{37}$$

3. Geometric and Shape Functions: ϕ and ρ, and F and G

The governing differential equations (26) and (27) discussed in section 2 are derived in polar co-ordinates system. However, the equation of non-circular shape is given in Cartesian co-ordinates as shown in Eq. (1). Therefore all variables related in geometric functions of ϕ and ρ in polar co-ordinates should be converted to the variables in Cartesian ones. Also, the shape functions of F and G related with the tapered arch should be converted. Now consider both the geometric and shape functions. First, the geometric functions ϕ and ρ are defined. The non-dimensional form for the parabolic arch shape given in Eq. (1) is obtained by using Eqs. (14), (15), (19) and (20). The result is

$$\eta = -4h\xi(\xi - 1), \quad 0 \le \xi \le e \tag{38}$$

By definition and by using Eq. (38), the following equations are obtained in term of single variable ξ.

$$\phi = \pi/2 - \tan^{-1}(d\eta/d\xi) = \pi/2 - \tan^{-1}[-4h(2\xi - 1)] \tag{39}$$

$$\rho = [1 + (d\eta/d\xi)^2]^{3/2}/(d^2\eta/d\xi^2) = (1/8)h^{-1}[1 + 16h^2(2\xi - 1)^2]^{3/2} \tag{40}$$

Also, by definition and by using Eqs. (39) and (40), the equations of ρ' and ρ'' are obtained as follows.

$$\rho' = (d\rho/d\xi)(d\xi/d\phi) = (3/2)(2\xi - 1)[1 + 16h^2(2\xi - 1)^2]^{3/2} \tag{41}$$

$$\rho'' = (d\rho'/d\xi)(d\xi/d\phi)$$
$$= (3/8)h^{-1}[1+64h^2(2\xi-1)^2]$$
$$\times[1+16h^2(2\xi-1)^2]^{3/2} \quad (42)$$

Second, the shape functions F and G are considered. Of the two basic classes of arched members[13], both the prime and quadratic arches are adopted here. The function G is derived for the prime arch. A prime arch is defined as an arch whose moment of inertia of cross-section varies in accordance with the prime equation of the arc length s:

$$I = I_f + (I_f - I_c)s/s_f \quad (43)$$

With Eqs. (16), (17) and (24), the above equation (43) becomes

$$I = I_f[\alpha + (1-\alpha)k^{-1}\mu] \quad (44)$$

in which the variable μ is defined already in Eq. (24) and can be obtained as follows.

$$\mu = \int [1+(d\eta/d\xi)^2]^{1/2}d\xi$$
$$= \int [1+16h^2(2\xi-1)^2]^{1/2}d\xi, \quad 0\le\xi\le e \quad (45)$$

It is noted that the integration of Eq. (45) can be performed by Simpson's rule used in this study and the k value defined in Eq. (16) is equal to the value of μ at $\xi = e$.

When Eqs. (3) and (44) are combined, the function of G can be expressed in terms of the variable μ. The result is

$$G = \alpha + (1-\alpha)k^{-1}\mu \quad (46)$$

in which the μ variable can be expressed in term of ξ as shown in Eq. (45).

When Eq. (46) are differentiated once and twice, the results are

$$G' = (1-\alpha)k^{-1}d\mu/d\phi$$
$$= (1-\alpha)k^{-1}\rho \quad (47)$$
$$G'' = (1-\alpha)k^{-1}\rho' \quad (48)$$

In last two equations, the ρ and ρ' are defined in Eqs. (40) and (41), respectively.

Similarly, the G, G' and G'' of quadratic arch are obtained as follows.

$$G = \alpha + (1-\alpha)k^{-2}\mu^2 \quad (49)$$
$$G' = 2(1-\alpha)k^{-2}\rho\mu \quad (50)$$
$$G'' = 2(1-\alpha)k^{-2}(\rho^2 + \rho'\mu) \quad (51)$$

Finally, the function F is defined for the cross-sectional shape. In this study, the cross-sectional shape is limited to the rectangular cross-section. The functions F and F' for rectangular cross-section are expressed in the form[14]

$$F = G^{\Gamma} \quad (52)$$
$$F' = \Gamma G^{\Gamma-1}G' \quad (53)$$

In Eqs. (52) and (53), the value of Γ is $\Gamma=1$ for the breadth taper, $\Gamma=1/2$ for the square taper, and $\Gamma=1/3$ for the depth taper.

As discussed above, all variables in section 2 can now be calculated from the single variable ξ, and consequently, the differential equations (26) and (27) can be solved in the Cartesian co-ordinates, not in the polar coordinates.

4. Numerical Methods and Computed Results

Based on the above analysis, a general FORTRAN computer program was written to calculate the frequency parameters $c_i(i=1,2,3,4)$ and the corresponding mode shapes $\delta=\delta_i(\xi)$ and $\zeta=\zeta_i(\xi)$, and the stress resultants $n=n_i(\xi)$, $q=q_i(\xi)$ and $m=m_i(\xi)$. The numerical methods described by Lee and Wilson[6], and Oh, et al.[2] were used to solve the differential equations (26) and (27), subjected to the boundary conditions of Eqs.(32)~(37). First, the determinant search method[15] combined with the Regula-Falsi method[16] was used to calculate the frequency parameters c_i, and then the Runge-Kutta method[16] was used to calculate the mode shapes. For given arch parameters h, α, λ, e, Γ and $R(=0$ or $1)$, the four lowest values of c_i and the corresponding mode shapes were calculated. The numerical results, given in Tables 1~3 and Figures 3~7, are summarized as follows.

In Table 1, comparisons are made between c_i

computed using the present analysis with $R=1$ and c_i computed with the packaged finite element program SAP 90. For latter calculations, 100 three-dimensional finite beam elements were used and effects of shear areas were not included. Comparing the results for like arch parameters, the results for c_i agree to within 2.5%. The remainder of the numerical results are based on the present analysis.

Table 2 shows the effect of rotatory inertia on the lowest four frequency parameters. The inclusion of rotatory inertia is to always depress the natural frequencies.

In Table 3, the effect of cross-sectional shapes on c_i is displayed. Here, the c_i value always increases as the cross-sectional shapes increase from breadth taper ($\Gamma=1$) to square taper ($\Gamma=1/2$) to depth taper ($\Gamma=1/3$).

Table 1 Comparison of results between this study ($R=1$)and finite element method(SAP 90)

Geometry	i	Frequency parameter, c_i	
		This study	SAP 90
h=0.3, α=3, λ=100, e=0.5, Γ=1/2, prime member	1	11.33	11.40
	2	68.64	69.19
	3	196.4	200.9
	4	307.2	307.7
h=0.4, α=2, λ=80, e=0.8, Γ=1, quadratic member	1	2.895	2.937
	2	18.85	19.10
	3	59.83	60.36
	4	117.6	119.6

Table 2 Effect of rotatory inertia on frequency parameter, c_i

Geometry*	R	Frequency parameter, c_i			
		i=1	i=2	i=3	i=4
λ=10, e=0.7	0	6.133	22.09	41.26	61.12
	1	5.798	22.00	40.83	59.79
λ=30, e=0.8	0	4.787	26.90	69.12	85.59
	1	4.764	26.52	68.00	81.92
λ=50, e=0.9	0	3.817	20.67	62.50	110.5
	1	3.812	20.59	61.60	110.0
λ=70, e=1.0	0	3.100	15.75	47.42	96.37
	1	3.099	15.73	47.15	95.25

* h=0.3, α=3, Γ=1/2, prime member

Table 3 Effect of cross-sectional shapes on frequency parameter, c_i

Geometry*	Γ	Frequency parameter, c_i			
		i=1	i=2	i=3	i=4
λ=20	1	5.600	30.28	54.67	84.59
	1/2	6.059	32.68	52.00	94.97
	1/3	6.212	33.25	51.41	98.50
λ=100	1	5.669	32.47	94.28	183.3
	1/2	6.148	36.47	108.9	212.1
	1/3	6.309	37.86	114.1	221.6

* h=0.3, α=3, e=0.7, R=1, prime member

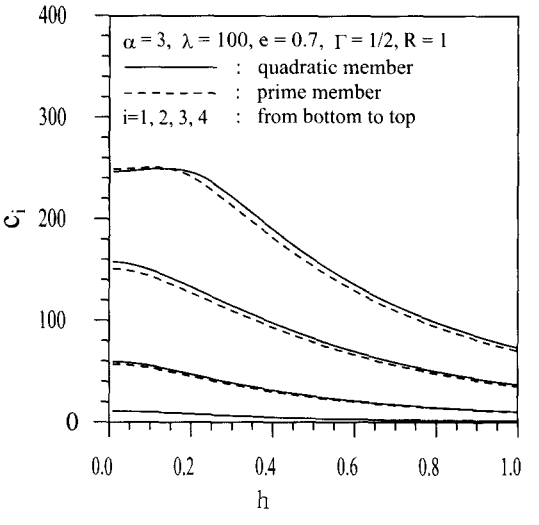

Fig. 3 c_i versus h curves

It is shown in Fig. 3, for which $\alpha=3$, $\lambda=100$, $e=0.7$, $\Gamma=1/2$(square taper), and $R=1$ for both the prime and quadratic members, that the frequency parameters $c_i(i=1,2,3,4)$ decrease as the rise to chord length ratio h is increased. Further, it is observed that the c_i values of quadratic member are greater than those of prime one. However, it is true that the fact is reversed for the 4th mode when the h value is less than about 0.2. Since the differences between the solid and dashed curves are very narrow, it is concluded that the effect of arched members on c_i may be negligible.

The results shown in Fig. 4 for $h=0.3$, $\lambda=100$, $e=0.7$, $\Gamma=1/2$ and $R=1$ depict the variation of $c_i(i=1,2,3,4)$ with the section ratio α. It is found

that the c_i values are increased as the α value increases. The increasing rate of c_i is higher at higher mode and especially that of first mode is relatively small comparing with the higher modes.

Figure. 5 shows the relationship between the $c_i(i=1,2,3,4)$ values and the slenderness ratio λ for $h=0.3$, $\alpha=3$, $e=0.7$, $\Gamma=1/2$ and $R=1$. It is seen that the c_i values increase, and in most cases approach a horizontal asymptote, as the λ value is increased. For the first mode, the effect of λ is very minor so that its effect is negligible.

It is shown in Fig. 6, for which $h=0.3$, $\alpha=3$, $\lambda=100$, $\Gamma=1/2$ and $R=1$, that the $c_i(i=1,2,3,4)$ values decrease as the span length to chord length ratio e is increased. The decreasing rate of each mode is very high when the e value is less than about 0.4.

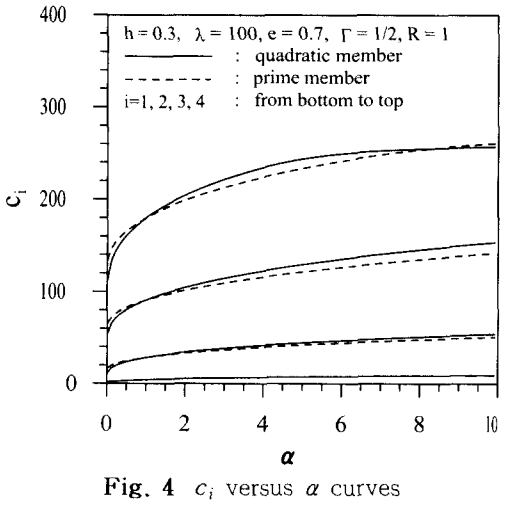

Fig. 4 c_i versus α curves

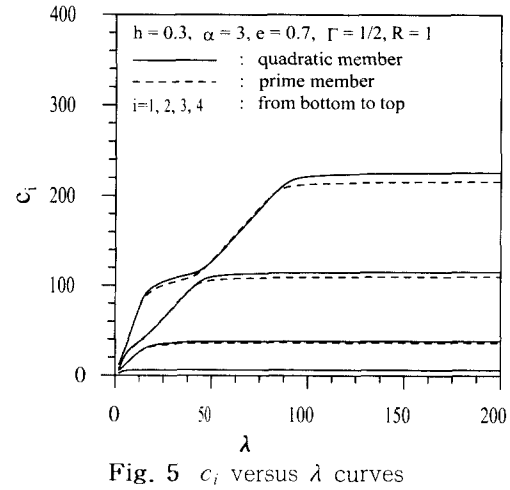

Fig. 5 c_i versus λ curves

Shown in Fig. 7 are the computed frequency parameters $c_i(i=1,2)$ and their corresponding mode (n, q, m) as well as displacements (δ, ζ) for which $h=0.3$, $\alpha=3$, $\lambda=100$, $e=0.7$, $\Gamma=1/2$, $R=1$and prime member. It is noted that for the axial load n, the first and second mode shapes are reversed with each other comparing with another modes.

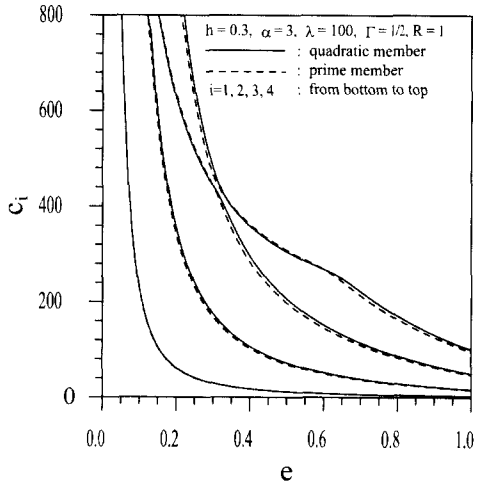

Fig. 6 c_i versus e curves

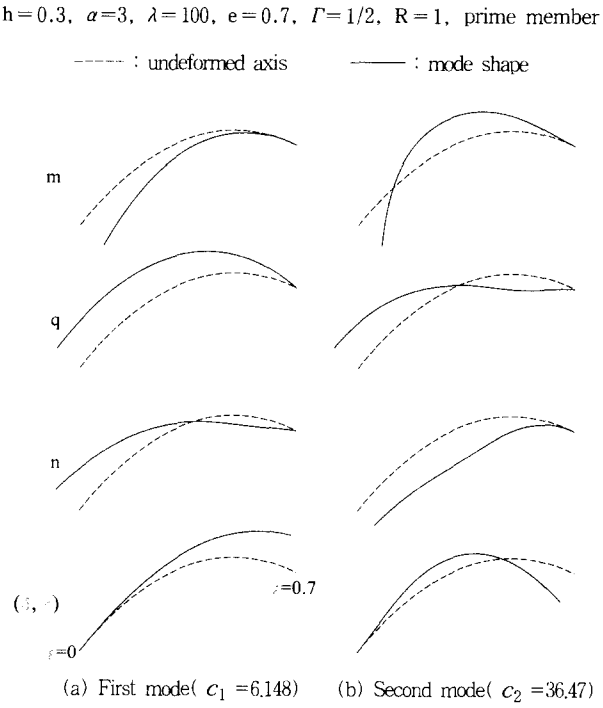

Fig. 7 Example of mode shapesshapes of stress resultants

5. Concluding Remarks

By employing the governing differential equations in Cartesian co-ordinates, the numerical methods for calculating the free vibration, in-plane frequencies and mode shapes for the tapered cantilever arches with variable curvature were found to be especially robust and reliable over a wide and practical range of arch parameters. The inclusion rotatory inertia was found to depress the natural frequencies. The c_i values increase as the cross-sectional shape increases from breadth to square to depth tapers. The effect of type of arched members on c_i is minor. The c_i values increase as both the α and λ values are increased while the c_i values decrease as both the h and e values are increased. The typical mode shapes of displacement (δ, ζ) as well as the stress resultants (n, q, m) are reported.

References

(1) Laura, P. A. A. and Maurizi, M. J., 1987, "Recent Research in the Vibration of Arch-like Structures," Shock and Vibration Digest, Vol. 19, No. 1, pp. 6~9.

(2) Oh, S. J., Lee, B. K. and Lee, I. W., 1999, "Natural Frequencies of Non-circular Arches with Rotatory Inertia and Shear Deformation," Journal of Sound and Vibration, Vol. 219, No. 1, pp. 23~33.

(3) Romanelli, E. and Laura, P. A. A., 1972, "Fundamental Frequencies of Non-circular, Elastic, Hinged Arcs," Journal of Sound and Vibration, Vol. 24, No. 1, pp. 17~22.

(4) Wang, T. M., 1972, "Lowest Natural Frequency of Clamped Parabolic Arcs," Journal of the Structural Engineering, ASCE, Vol. 98, No. ST1, pp. 407~411.

(5) Wang, T. M. and Moore, J. A., 1973, "Lowest Natural Extensional Frequency of Clamped Elliptic Arcs," Journal of Sound and Vibration, Vol. 30, pp. 1~7.

(6) Lee, B. K. and Wilson, J. F., 1989, "Free Vibrations of Arches with Variable Curvature," Journal of Sound and Vibration, Vol. 36, No. 1, pp. 75~89.

(7) Royster, L. H., 1966, "Effect of linear Taper on the Lowest Natural Extensional Requency of Elastic Arcs," Journal of the Applied Mechanics, ASME, Vol. 33, pp. 2111~2112.

(8) Laura, P. A. A. and Verniere de Irassar, P. L., 1988, "A Note on Vibrations of a Circumferential Arch with Thickness Varying in a Discontinuous Fashion," Journal of Sound and Vibration, Vol. 120, No. 1, pp. 95~105.

(9) Sakiyama, T., 1988, "Free Vibration of Arches with Variable Cross-section and Non-symmetric Axis," Journal of Sound and Vibration, Vol. 102, pp. 448~452.

(10) Wilson, J. F., Lee, B. K. and Oh, S. J., 1994, "Free Vibrations of Circular Arches with Variable Cross-section," Structural Engineering and Mechanics, Vol. 2, No. 4, pp. 345~357.

(11) Irie, T., Yamada, G. and Tanaka, K., 1983, "Natural Frequencies of In-plane Vibration of Arcs," Journal of the Applied Mechanics, ASME, Vol. 50, pp. 449~452.

(12) Borg, S. F. and Gennaro, J. J., 1959, Advanced Structural Analysis, Van Nostrand, New Jersey.

(13) Leontovich, V., 1969, Frames and Arches, McGraw-Hill.

(14) Gupta, A. K., 1985, "Vibration of Tapered Beams," Journal of the Structural ngineering, ASCE, Vol. 111, pp. 19~36.

(15) Leonard, J. W., 1988, Tension Structures, McGraw-Hill.

(16) Al-Khafaji, A. W. and Tooley, J. R., 1986, Numerical Method in Engineering Practice, Holt, Reinhardt and Winston, Inc.